Organic Electronics 11 (2010) 1668–1675

Contents lists available at ScienceDirect

Organic Electronics

journal homepage: www.elsevier.com/locate/orgel

Synchronous vapor-phase polymerization of poly(3,4-ethylenedioxythiophene) and poly(3-hexylthiophene) copolymer systems for tunable optoelectronic properties

Keon-Soo Jang [a,b], Dong Ouk Kim [c], Jun-Ho Lee [a], Seung-Chul Hong [a], Tae-Woo Lee [d], Younkwan Lee [e], Jae-Do Nam [a,*]

[a] Department of Energy Science and Department of Polymer Science and Engineering, Sungkyunkwan University, Suwon 440-746, Republic of Korea
[b] Polymer Hybrid Research Center, Korea Institute of Science and Technology Seoul 130-650, Republic of Korea
[c] Department of Chemistry, Stanford University, Stanford, CL 94305, USA
[d] Material Science and Engineering, Pohang University of Science and Technology, Pohang, Republic of Korea
[e] Department of Chemical Engineering, Sungkyunkwan University, Suwon 440-746, Republic of Korea

ARTICLE INFO

Article history:
Received 11 February 2010
Received in revised form 30 May 2010
Accepted 7 July 2010
Available online 14 August 2010

Keywords:
Poly(3-hexylthiophene) (P3HT)
Poly(3,4-ethylenedioxythiophene) (PEDOT)
Vapor-phase polymerization (VPP)
Thin copolymer film
Conducting polymer

ABSTRACT

We successfully copolymerized poly(3,4-ethylenedioxythiophene) and poly(3-hexylthiophene) (PEDOT and P3HT) synchronously polymerizing two monomers in the vapor phase to give tunable bandgap, conductivity, surface morphology and water contact angles. Due to different vapor pressures and polymerization rates of the monomers, the PEDOT to P3HT ratios were kinetically controlled by adjusting the feed concentrations of monomers to the polymerization reaction chamber. Depending on the compositions of the two polymer systems, the optical bandgap of the thin PEDOT/P3HT copolymer film was controlled successfully in the 575–650 nm range. In addition, the electrical conductivity, surface roughness and water contact angle of the vapor-phase polymerized PEDOT/P3HT copolymer system changed in the range of 3.0×10^{-2}–2.3×10^{1} S/cm, 4.9–18.3 nm, and 34–54°, respectively, correlated with the altered composition of two polymers. Tailoring the bandgap and other optoelectronic properties, the copolymerized P3HT/PEDOT film can provide tunable properties to be used not only as a hole injection layer (HIL) in organic light-emitting diodes (OLEDs) but also as a semiconductor with improved mobility in organic thin film transistors (OTFTs) and organic photovoltaics (OPVs).

1. Introduction

Since conducting polymers (CP) were first reported, poly(3,4-ethylenedioxythiophene) (PEDOT) is arguably one of the most commercially useful and most studied CPs in the last 20 years [1–7]. PEDOT has been studied extensively on account of its many advantageous properties, such as high electrical conductivity, good transmittance and thermal stability with a low optical bandgap and thermal stability [4,6]. These properties make PEDOT very attractive for applications, such as electrochromic windows [8], organic electrodes for organic photovoltaic cells (OPVs) [9,10] and hole injection layers (HIL) in organic light emitting devices (OLEDs) [11–14] and dye-sensitized solar cells [15]. In particular, PEDOT is commonly used as a hole extraction layer in OPVs [16,17]. In most optoelectronic applications as a buffer or electrode layer, the bandgap of the layer plays an important role in determining the operating characteristics, quantum efficiency and electron/hole transport. Therefore, the main issues for electronic device applications include both the electrical conductivity and bandgap.

Oxidized PEDOT can be produced in a variety of forms using different polymerization techniques. Solution

* Corresponding author. Tel.: +82 31 290 7285; fax: +82 31 292 8790.
E-mail address: jdnam@skku.edu (J.-D. Nam).

1566-1199/$ - see front matter © 2010 Elsevier B.V. All rights reserved.
doi:10.1016/j.orgel.2010.07.006

processing is used most commonly in synthesizing PEDOT in the form of spin-coating, solvent-casting or ink-jet printing. However, these PEDOT systems are relatively insoluble in most solvents, making it necessary to attach soluble functional groups to the polymer or dope it with stabilizing polyelectrolytes [18]. An aqueous dispersion of poly(3,4-ethylenedioxythiophene)-poly(styrenesulfonate) (PEDOT-PSS), commercially available as Baytron P, is a stable polymer system with a high transparency up to 80% [7]. However, the PEDOT-PSS film exhibits relatively low electrical conductivity, 10–500 S/cm [7], which does not often meet the high conductivity required for most applications. In addition, scanning-tunneling microscopy, neutron reflectivity measurements, and X-ray photoelectron spectroscopy have revealed a PSS rich layer on the top of the spin-coated PEDOT-PSS films due to the phase separation [13,19,20]. Since PSS is an electrical insulator, excessive PSS can limit the film conductivity [19], and an acidic PEDOT-PSS dispersion can etch indium tin oxide (ITO) during the polymer spin-coating process. Moreover, the hydrolysis of the deposited PEDOT-PSS by moisture absorption can also etch ITO to cause indium and tin incorporation into the polymer [14].

For the PEDOT systems without using polyelectrolytes, PEDOT can be deposited directly on the substrate surface by several in situ polymerization techniques. One of the options is electrochemical polymerization, which has been reported to have higher electrical conductivity [21]. However, electrochemical polymerization results in a poor transparency and requires conducting substrates, which limits its practical applications. As an alternative, oxidative chemical polymerization either in the liquid or vapor phase is more versatile because it is not restricted by the substrates. In particular, one way of achieving a clear thin film with a smooth surface is to apply the oxidant using solvent coating processes and expose the coated surface to a reactive monomer vapor. This process is often referred to as vapor-phase polymerization (referred to herein as VPP) [4,5,22–26]. The PEDOT films by VPP have been reported to have conductivities of approximately 15 S/cm at a thickness of 300 nm without any additives [22]. Recently, a PEDOT film with high conductivity, exceeding 1000 S/cm, was reported using a base-inhibited VPP [3,4]. However, it should be noted that VPP PEDOT has a high bandgap and relatively low transmittance [23,24].

As another thiophene-based conducting polymer, poly(3-hexylthiophene) (P3HT) is also one of the most indispensable materials in OLEDs, OPVs, field effect transistors (FETs) and thin film transistors (TFTs) [12,17,27,28]. Over the last decade, blending or copolymerization techniques of conducting polymers have been investigated not only to overcome the drawbacks of a pristine conductive polymer, such as inadequate bandgap, rough surface, low conductivity and poor transmittance, but also to tailor the properties for various applications [29–31]. Recently, P3HT has been successfully fabricated by VPP [32] using a similar route to VPP of PEDOT choosing appropriate catalyst and solvent systems. Using the VPP technique, therefore, PEDOT and P3HT may be copolymerized in the state of vaporized monomers and subsequently polymerized to form, most probably, a PEDOT/P3HT copolymer structure. However, it should be mentioned that the traditional VPP route, where the monomer is maintained in the state of thermodynamic equilibrium, may not simply be applied because the vapor pressure and polymerization rate of the EDOT and 3HT are different and, thus, the relative composition of the VPP copolymer is not controllable.

Therefore, the PEDOT to P3HT ratio was kinetically controlled in this study by adjusting the relative feed amount of the evaporating monomers to the reaction chamber to fabricate the PEDOT/P3HT films containing different ratios of PEDOT to P3HT. The developed synchronous VPP technique successfully provided PEDOT/P3HT copolymer thin coatings with tunable bandgap and optoelectronic properties.

2. Experimental method

The main chemicals used in this study were 3HT (99%, Aldrich, St. Louis, MI USA), EDOT (99%, Aldrich, St. Louis, MI USA), iron (III) chloride hexahydrate ($Fe(III)Cl_3{\cdot}6H_2O$, 97%, Aldrich, St. Louis MI USA), MeOH (methyl alcohol anhydrous, 99.9%, Carlo erba reagenti) and EtOH (ethyl alcohol anhydrous, 99.9%, Carlo erba reagent). The substrate materials used in this study were plane glass (1.1 mm, Paul Marienfeld GmbH & Co. KG., Germany), ITO glass (indium–tin-oxide glass, 10 Ω, 185 ± 20 nm ITO thickness, 1.1 mm ITO glass thickness, U. I. D., Korea), PET (polyethylene terephthalate, 100 μm, Hwasung Co. Ltd., Korea) and a Si wafer (Thickness: 525 ± 25 μm, SEMI-MATERIAS Co. Ltd., Korea).

The substrates were washed and rinsed with DI-water and acetone and sonicated for 10 min to remove any organic contaminants. The glass substrates were plasma-treated (PLAMAX, SPS Co. Ltd., Korea) for 30 s, and the ITO glass substrates were UV-treated for 20 min. The oxidant was a mixture of MeOH and EtOH at a 1:1 ratio with iron (III) chloride hexahydrate. The wt.% ratio between the alcohol mixture and $FeCl_3 \cdot 6H_2O$ was 10:1, 5:1, and 3:1. A ratio of 10:1 was chosen to fabricate most thin films in this study. After sonicating the oxidant solution for 2 min at 40 °C, it was spin-coated onto the substrates at a speed of 500 rpm for 5 s and then at 1400 rpm for 5 s. The oxidized substrates were placed in the vapor-phase-polymerization (VPP) chamber, where the containers of 3HT and EDOT were also placed. The vaporized monomers were supplied into the chamber through the feed inlets, which were made at the center of the container ceiling with different inlet diameters of D_{3HT} and D_{EDOT} (Scheme 1). The flow rate of flowing nitrogen was kept constant during polymerization, and the feed ratio of 3HT and EDOT monomer vapors was adjusted by the inlet diameters of D_{3HT} (0, 2, 4, 6, and 8 mm) and D_{EDOT} (fixed at 20 mm). The EDOT and 3HT monomers in the VPP chamber were polymerized for 20 min, 30 min, or 1 h at 60 °C. After polymerization, the sample was soaked and washed sequentially with MeOH to eliminate the monomers and Fe(III) solution remaining on the substrate. The washed PEDOT/P3HT copolymer film was dried further using a hot-air gun for 1 min in an ambient atmosphere to remove the residual MeOH.

The thickness of the VPP PEDOT/P3HT was measured using an alpha step IQ (KLA Tencor corporate, the Yield Management company, San Jose CA, U. S. A.) and FE-SEM (Field emission scanning electron microscope, 1.0 nm guaranteed at 15 kV, JSM6700F, JEOL, Japan). The bandgap was determined by UV–vis-spectrophotometry (UV-3600, SHIMADZU, Japan). AFM (SPA-300HV, SII Nano Technology Inc., Tokyo Japan) was used to examine the surface morphology of the VPP-PEDOT/P3HT coating, where a 5×5 μm area was analyzed to determine the surface roughness. The AFM 3D images revealed the surface roughness of the copolymer films with a *z*-axis of 100 nm. X-ray photoelectron spectroscopy (XPS, ESCA2000, VG MICROTECH) equipped with an Al Kα radiation source ($h\nu = 1486.6$ eV) was used to analyze the components. Attenuated total reflection-Fourier transform infrared (ATR-FTIR) spectroscopy (Bruker IFS-66/S, Bruker, Massachusetts U.S.A.) was also used for component analysis of the VPP-PEDOT/P3HT copolymers. Contact angle measurements were performed using a Digi-drop contact angle goniometer (JinTech, Korea). A water droplet was dropped onto the surface of a small sample. The droplet shape was recorded by a camera and analyzed to determine the contact angle. The electrical conductivity of the synthesized films was measured using a four-point probe method (Keithley 236 current source and Keithley 617 electrometer). The film thickness for the measurement of electrical conductivities ranged 100–500 nm coated on a glass substrate in the area of 25×25 mm^2. The type of the four-probe point was a linear type with 1 mm tip spacing.

3. Results and discussion

The thin copolymers were fabricated by adding a small amount of EDOT monomer in the VPP chamber with excessive 3HT monomers because the polymerization rate of the EDOT monomers was faster than that of the 3HT monomers. More specifically, the composition was controlled by adjusting the feed amount of EDOT to the catalyst-coated layer placed in the reaction chamber, which complies with the typical steady-state plug-flow reactor system [33]. In this case, the feed ratio of EDOT to 3HT may be controlled by the inlet size of the vaporized monomers in the stream of purging nitrogen. Simply quantifying the feed composition, the feed ratio (r) may be defined by the feed inlet sizes of EDOT and 3HT, viz: $r = D_{EDOT}/D_{3HT}$, where D_{EDOT} and D_{3HT} are the cross-sectional diameters of the feeding hole on the ceiling of the EDOT and 3HT containers, respectively.

The ATR-FTIR spectroscopy results of the pristine PEDOT, pristine P3HT and PEDOT/P3HT copolymer films are compared in Fig. 1 at different feed ratios. As the characteristic peaks of each pristine polymer, the peak intensity of the aliphatic C–H bond stretching vibration corresponds to the 3-hexyl group in P3HT, and the C–O–C bond stretching vibration corresponds to the ethylenedioxy group in PEDOT. As seen in Fig. 1B, the aliphatic C–H bond stretching in the 3-hexyl group in P3HT appears at 2854, 2924, and 2954 cm^{-1}, and its peak intensity decreases with the feed ratio of r [34,35]. Assigning the bands at approximately 1058 and 1141 cm^{-1} to the stretching modes of the ethylenedioxy group [36,37], the intensity of these peaks increases with the increasing supply of the EDOT monomer. Consequently, the vapor-phase polymerization ratio of PEDOT appears to reflect the controlled supply of the EDOT monomer via the feed ratio of r. Fig. 1C compares the bands of the pristine PEDOT (doped with $FeCl_3 \cdot 6H_2O$) with the copolymers at different feed ratios of r, seemingly exhibiting a redshift due to copolymerization of 3HT and EDOT. The inset in Fig. 1A shows the camera images of pristine PEDOT, P3HT, and PEDOT/P3HT at different compositions coated on the ITO substrates. Since the colors of the pristine PEDOT and P3HT are blue and orange, respectively, the color of the PEDOT/P3HT copolymers changes gradually from orange to dark blue with the increasing EDOT feed ratio of r demonstrating that the ratio was successfully controlled by the feed ratio in our experiments.

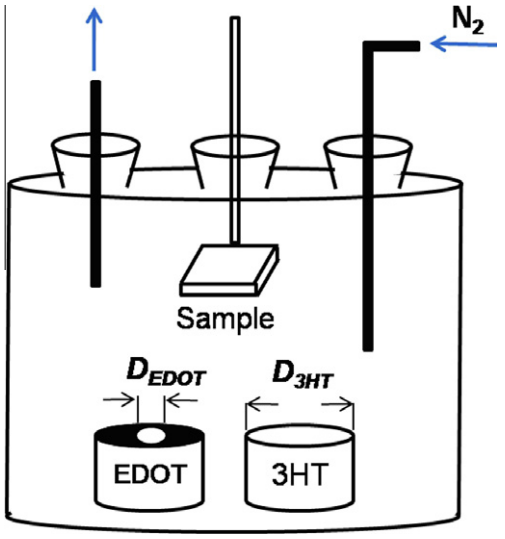

Scheme 1. Schematic of experimental setup for synchronous polymerization of EDOT and 3HT monomers, where the monomer concentrations are controlled by the inlet sizes of monomers (D_{EDOT} and D_{3HT}) to the reaction chamber under the flowing inert gas.

For copolymers, the surface composition may be quantified using several surface-sensitive techniques, such as XPS and time-of-flight secondary ion mass spectrometry (ToF-SIMS) [38], XPS exhibiting somewhat better agreement with the theoretical compositions than ToF-SIMS [39]. Therefore, in this study, XPS was used to quantify the surface concentrations. The formation of PEDOT/P3HT copolymer films can be demonstrated by deconvoluting the XPS peaks at 285.0, 286.5, and 533.0 eV, as shown in Fig. 2. The XPS peaks at 285.0 and 286.5 eV in Fig. 2A can be assigned to C–C/C =C and C–O–C, respectively, corresponding to the spectra of the C(1s) core level [40,41]. Fig. 2A and Table 1 indicate that the intensity of the peak at 285.0 eV decreases with increasing r, whereas that at 286.5 eV increases, which agrees well with the chemical structures of PEDOT and P3HT, as shown in the inset in Fig. 2A. The O photoelectron spectrum in Fig. 2B and Table 1 shows that the O concentration increases with increasing r, as represented by the intensities of the XPS peak at

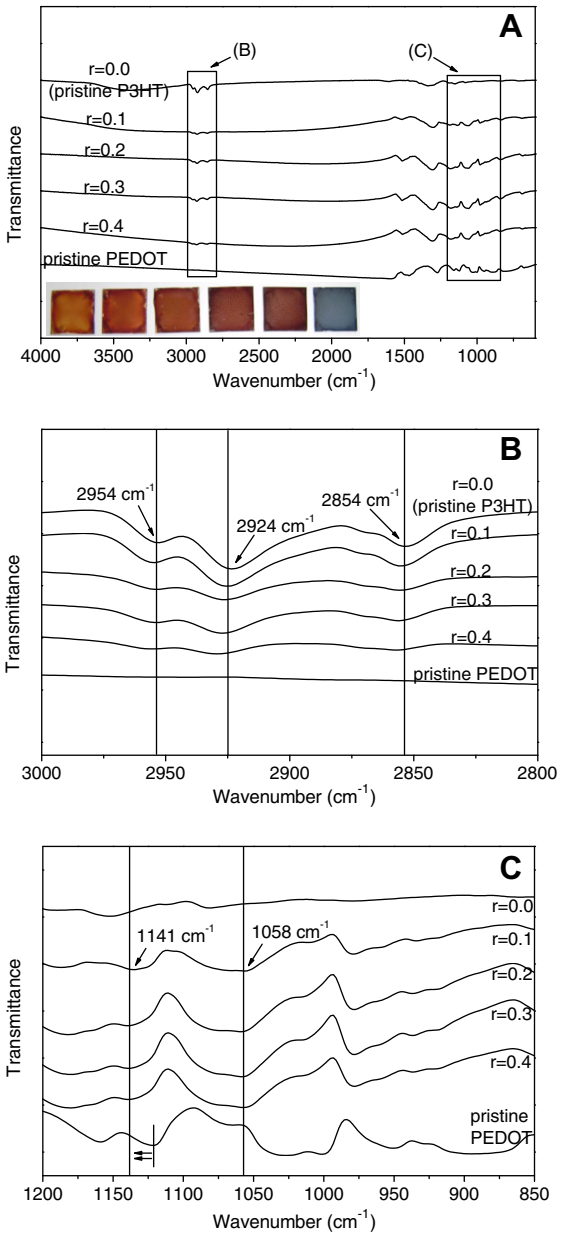

Fig. 1. Comparison of ATR-FTIR spectra of the PEDOT/P3HT copolymers at different feed ratio of *r*. (A) full spectral region: 4000–600 cm^{-1}, (B) enlargement of the region of 3000–2800 cm^{-1}, (C) enlargement of the region of 1200–850 cm^{-1}. The inset in (A) shows pictures of the PEDOT/P3HT copolymer films coated on ITO-coated glass using an oxidant at a 5:1 ratio of the alcohol mixture to ferric chloride hexahydrate, representing $r = 0$, 0.1, 0.2, 0.3, 0.4, and the pristine PEDOT film from left to right, respectively, with a thickness of 500 nm.

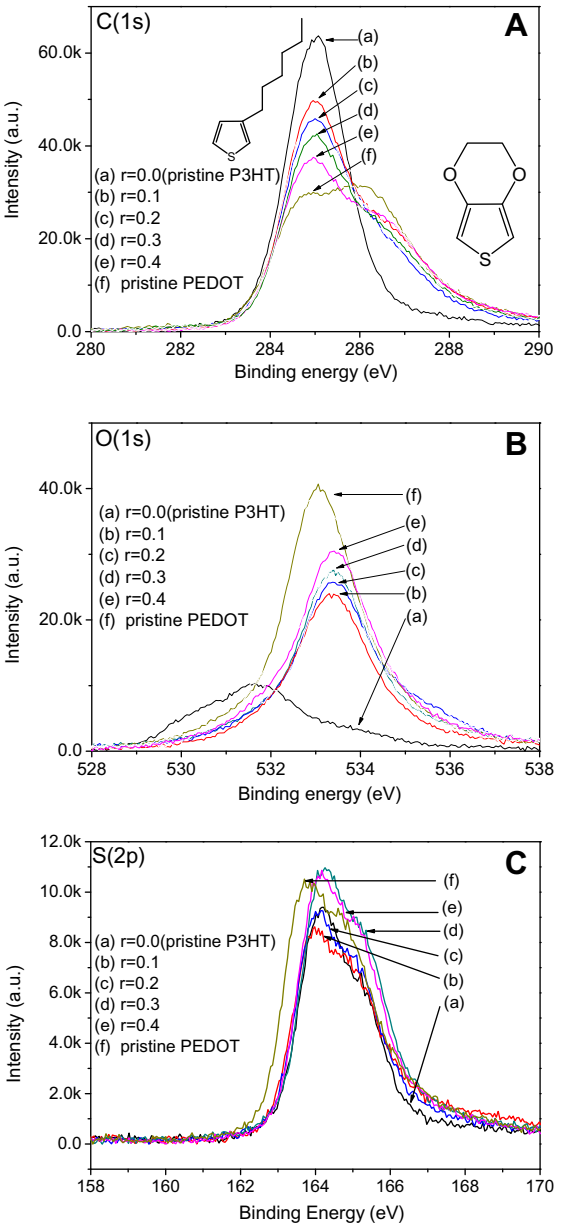

Fig. 2. Deconvolution of XPS spectra of (A) $C_{(1s)}$, (B) $O_{(1s)}$ core-level, and (C) $S_{(2p)}$ for PEDOT/P3HT copolymers at various feed ratio of *r*. The inset in (A) is chemical structures of PEDOT and P3HT, respectively.

533 eV, which can be assigned to the oxygen–ether group (C–O–C) [40,42]. The S photoelectron spectrum is shown in Fig. 2C and analyzed in Table 2. The S(2p) peak positions of pristine P3HT and PEDOT appear at 164.1 and 163.8 eV, respectively, and the peaks of their blend systems at different *r* values seem to appear between the two pristine polymers. Table 2 shows the elemental composition of the fabricated thin films demonstrating that the PEDOT to P3HT ratio increases with the EDOT feed ratio of *r*. As seen in Table 2, the concentration of S and the PEDOT to P3HT elemental ratio apparently increase with increasing *r*. Comparing the experimental and theoretical ratios of C/S, which may represent the ratios of P3HT to PEDOT, there are good agreements between the theoretical and experimental values. The slight discrepancy might be due to adventitious hydrocarbon contamination coming from the contact of the samples with the ambient atmosphere [39].

Table 1
XPS atomic concentrations (%) of C and O for PEDOT/P3HT copolymers with (a) $r = 0.0$, (b) 0.1, (c) 0.2, (d) 0.3, (e) 0.4, and (f) pristine PEDOT.

Samples	C(1s) C atom% at (g) 285.0 eV (C–C/C=C)	(h) 286.5 eV (C–O–C)	h/g	O(1s) O atom% at 533.0 eV (C–O–C)
a	78.4	0	0	0
b	50.0	24.6	0.49	8.6
c	48.1	25.9	0.54	9.1
d	42.4	28.4	0.67	10.4
e	35.1	28.9	0.82	11.6
f	29.2	32.1	1.10	13.8

Table 2
XPS atomic concentrations (%) of C and S comparing C/S ratios between theoretical and experimental results for (a) $r = 0.0$, (b) 0.1, (c) 0.2, (d) 0.3, (e) 0.4, and (f) pristine PEDOT.

Samples	C(1s) atom%	S(2p) atom%	C/S theoretical	C/S experimental	PEDOT:P3HT experimental ratio(mol%)
a	84.1	8.2	10.0	10.3	0:100
b	80.4	8.7	–	9.2	31:69
c	78.4	8.8	–	8.9	39:61
d	75.4	9.7	–	7.8	69:31
e	74.8	9.9	–	7.5	78:22
f	69.5	10.4	6.0	6.7	100:0

Fig. 3 presents the UV–vis absorbance spectra of VPP-PEDOT/P3HT films on glass substrates leading to changes of the bandgap of the VPP-PEDOT/P3HT copolymer at different feed ratio of r values. The bandgap was estimated to be 1.91, 1.98, 2.02, 2.07, and 2.16 eV for the specimens prepared with 0, 2, 4, 6 mm of feed diameters and the pristine VPP-PEDOT film, respectively, by taking the isobestic points at 650, 625, 615, 600, and 575 nm, respectively. The bandgap decreases gradually with decreasing EDOT monomer supply. Accordingly, the bandgap of the VPP-PEDOT/P3HT copolymer film can be desirably adjusted by changing the relative composition of PEDOT and P3HT, especially when a low bandgap is required in such applications as OLEDs and OPVs [16]. The inset in Fig. 3 shows the pristine PEDOT, P3HT and PEDOT/P3HT copolymers at different compositions coated on glass substrates. Similarly to Fig. 1, the color of the specimens clearly indicates that the compositions of PEDOT and P3HT vary with the fabrication conditions to give tunable bandgap.

Fig. 4 shows cross-sectional SEM images of pristine PEDOT, P3HT, and copolymerized PEDOT/P3HT films produced by the developed synchronous technique. In this experiment, the coating thickness of the oxidant was precisely controlled to be constant during the spin-coating process and the same VPP conditions were used. However, as can be seen, the final film thickness varies with the compositions because of the difference in polymerization rates of EDOT and 3HT. Fig. 4A, B, C, D, E and F show cross section images of pristine P3HT, copolymer films and pristine PEDOT, giving the final thicknesses of 52, 71, 87, 110, 131 and 153 nm at $r = 0$, 0.1, 0.2, 0.3, 0.4 and the pristine PEDOT film, respectively. The film thickness increases with increasing r due to the faster polymerization rates of EDOT than 3HT. It should be mentioned that the film thickness can also be controlled at a fixed r by changing the polymerization temperature [32].

Fig. 5 shows the electrical conductivity of the copolymers plotted as a function of r. The electrical conductivity increases from 3.0×10^{-2} S/cm for the pristine P3HT up to 6.28 S/cm for the copolymer with r at 0.4. The conductivity of PEDOT/P3HT copolymer can be increased up to 200 times higher than that of the pristine P3HT, which can be achieved by adjusting the EDOT feed ratio of r. In this study, the conductivity of the pristine VPP-PEDOT was similar to that reported elsewhere [22], where a $FeCl_3$-based oxidant solution was used without any additives. However, the addition of basic inhibitors, such as pyridine [4] and imidazole [25], has been reported to reduce the polymerization reaction kinetics and enhance the conductivity and transparency of the PEDOT film. Therefore, a weak base can be used to the PEDOT/P3HT copolymer systems to

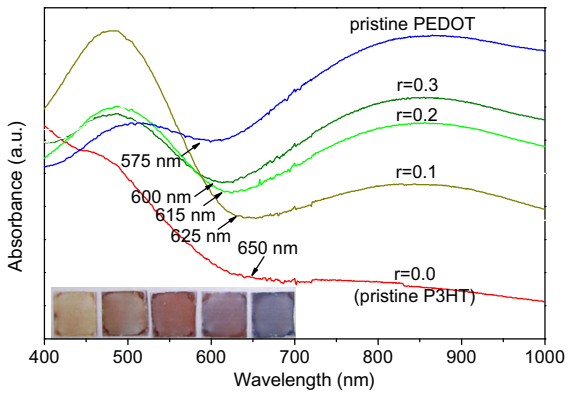

Fig. 3. UV–vis. absorbance spectra of the various PEDOT/P3HT copolymer films. The inset shows pictures of the PEDOT/P3HT copolymer films coated on ITO-coated glass using an oxidant at a 10:1 ratio of mixture to ferric chloride hexahydrate, representing $r = 0$, 0.1, 0.2, 0.3, 0.4, and the pristine PEDOT film from left to right, respectively, with a thickness of 300 nm.

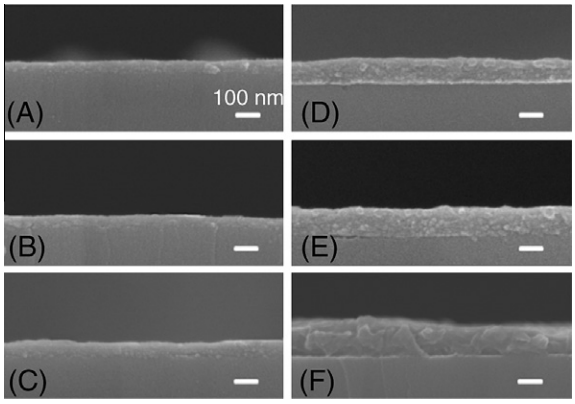

Fig. 4. Cross section of the PEDOT/P3HT copolymer films for (A) $r = 0.0$ (pristine P3HT), (B) $r = 0.1$, (C) $r = 0.2$, (D) $r = 0.3$, (E) $r = 0.4$ and (F) pristine PEDOT synthesized at 60 °C for 20 min. The scale bar is 100 nm in each.

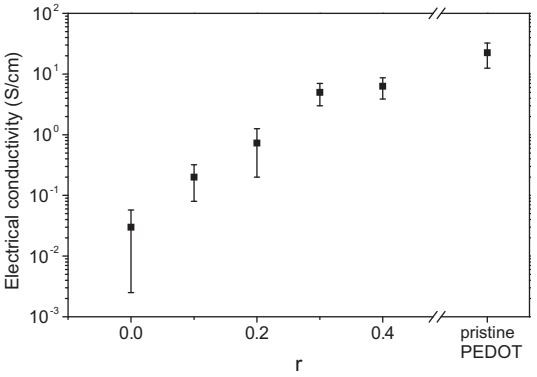

Fig. 5. Electrical conductivities of the pristine PEDOT, P3HT, and PEDOT/P3HT copolymer films.

achieve high conductivities, which is desirable for electrode systems in various electronic devices.

The polymerization rate of conjugated polymers, surface treatment and catalyst removal conditions were reported to affect the surface morphology of thin films substantially [5]. For example, the residual catalyst and monomers were removed successfully in order to synthesize smoother thin conducting polymer films [26]. Fig. 6 shows the surface morphology of the VPP-PEDOT/P3HT thin films in different polymerization conditions at different EDOT feed ratios of *r*. The surface roughness of the film increases with increasing *r*, as shown in Fig. 6A, B, C, D, and E, giving a RMS roughness of 4.88, 3.83, 8.66, 9.31, and 9.54 nm for $r = 0$, 0.1, 0.2, 0.3, and 0.4, respectively. This demonstrates that the surface roughness is affected by the incorporated EDOT monomers. The copolymerized film with $r = 0.1$ shows a lower RMS roughness than the pristine P3HT film (4.88 nm). However, the RMS roughness of the copolymer films increases gradually up to 18.3 nm with increasing *r*. The surface roughness of the pristine PEDOT is relatively high (ca. 18.3 nm) in Fig. 6F because no additional dopant was used in this study. Various additives are normally used to improve both conductivity and surface morphology of PEDOT, for example, such as glycerol, sorbitol and pyridine [5,43]. It should also be mentioned that $FeCl_3$ readily forms crystal-like structures as the

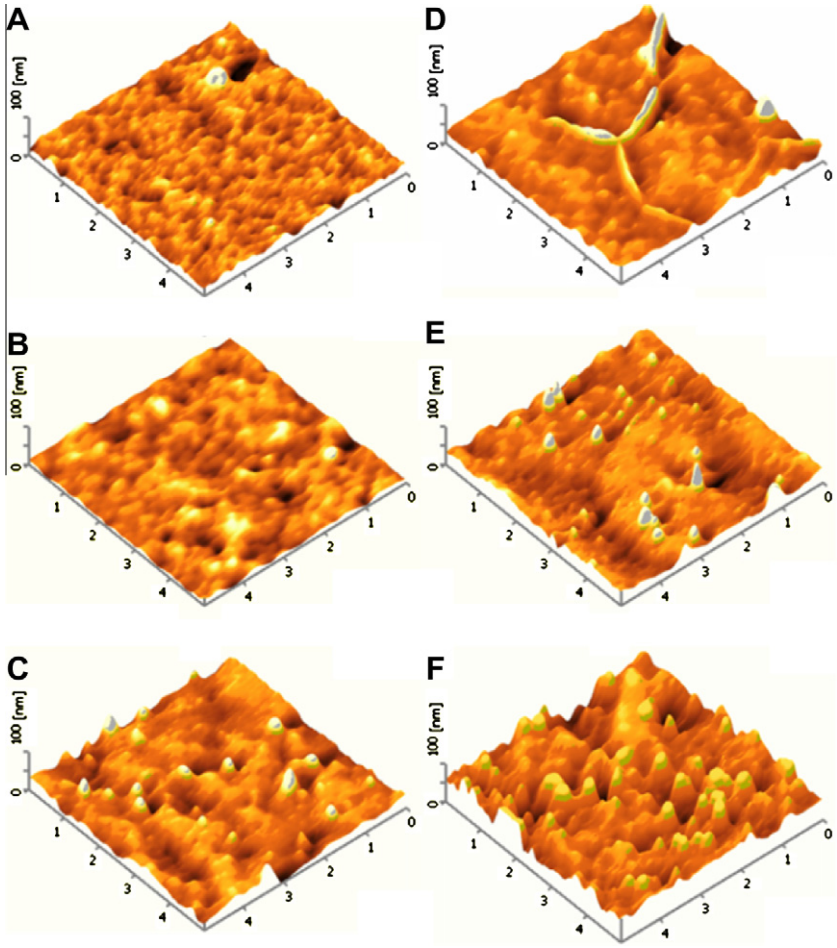

Fig. 6. AFM images of PEDOT/P3HT copolymers for (A) $r = 0.0$ corresponding to pristine P3HT, (B) $r = 0.1$, (C) $r = 0.2$, (D) $r = 0.3$, (E) $r = 0.4$ and (F) pristine PEDOT.

solvent evaporates to give grainy structures, which may act as a seeding template to cause discontinuous film formation [26]. Further work by Winther-Jensen et al. [4,26] shows that Fe(III) tosylate gives relatively smooth and homogeneous film surfaces, however, which often results in an undesirable polymerization route to give partially conjugated polymer chains. Therefore, further study of different additives and catalysts should be performed to enhance the surface morphology of VPP-PEDOT/P3HT.

Fig. 7 shows the water contact angle and RMS surface roughness of the copolymerized films coated on the glass substrates. Since a liquid makes contact with the outermost molecular layer of a surface, the contact angles represent the chemical and structural differences at the coating surface. Furthermore, the wettability of the thin coating is important in the fabrication of many optoelectronic devices, where multilayers should be fabricated in contact with heterogeneous layers. Since the contact angle of the pristine PEDOT at 36° is lower than that of the pristine P3HT at 54°, the PEDOT/P3HT copolymer films show a decreasing feature of the contact angle with a higher *r*, which is likely affected by the roughness of the coating since the water contact angle usually decreases with increasing RMS roughness. At a feed ratio of $r = 0.4$, however, the contact angle is slightly lower than the pristine PEDOT. Exhibited by the camera images of coating in the insets of Fig. 7, the color changes gradually from yellow to blue with the increasing EDOT feed ratio of *r*.

Overall, the developed VPP copolymerizing technique clearly demonstrates that the physicochemical properties of PEDOT/P3HT copolymers were successfully adjusted. Since the vapor pressure and polymerization rates of EDOT and 3HT monomers are different, the variation of the copolymer composition was ensured by adjusting the feed ratio of the monomers to the reaction chamber, which resulted in different reactant concentrations of EDOT and 3HT monomers. Different concentrations of reactants may well give different kinetic polymerization rates of EDOT and 3HT to provide a controllable synthesis route of PEDOT/P3HT copolymer coatings. Further study should be performed to identify the detailed copolymerization reaction and chemical structures of the VPP PEDOT/P3HT copolymer system.

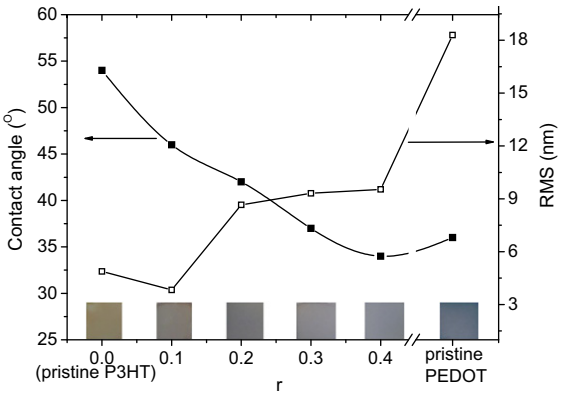

Fig. 7. Water contact angles and RMS surface roughness for different PEDOT/P3HT films. The inset shows the camera images of PEDOT/P3HT copolymer films with thickness of ca. 100 nm.

4. Conclusions

PEDOT/P3HT copolymer films were successfully fabricated as thin films on the glass, Si wafer, ITO-covered glass and PET film substrates using a vapor-phase polymerization technique. The ratios were kinetically controlled to ensure the tunable properties of bandgap, electrical conductivity, surface morphology and water contact angle of the thin copolymer films. The P3HT thin film incorporated with PEDOT may improve the mobility in OTFTs and charge extraction efficiency in OPVs. In addition to being used as a semiconductor with higher mobility, adding dopants to increase the electrical conductivity, P3HT/PEDOT copolymer films can also be used as a HIL in OLEDs with modified energy levels and properties.

Acknowledgments

This research was supported by WCU (World Class University) program through the Korea Science and Engineering Foundation funded by the Ministry of Education, Science and Technology (R31-2008-000-10029-0). The authors wish to express their gratitude for the project and equipment support from Gyeonggi Province and Samsung Electro-mechanics Co. through the GRRC program in Sungkyunkwan University.

References

[1] H. Shirakawa, E. Louis, A. MacDiarmid, C. Chiang, A. Heeger, J.S.C. Chem. Commun. 1977 (1977) 578–580.
[2] C.K. Chiang, C.R. Fincher, Y.W. Park, A.J. Heeger, H. Shirakawa, E.J. Louis, S.C. Gau, A.G. MacDiarmid, Phys. Rev. Lett. 39 (1977) 1098.
[3] B. Winther-Jensen, M. Forsyth, K. West, J. Andreasen, G. Wallace, D. MacFarlane, Org. Electron. 8 (2007) 796–800.
[4] B. Winther-Jensen, K. West, Macromolecules 37 (2004) 4538–4543.
[5] T. Truong, D. Kim, Y. Lee, T. Lee, J. Park, L. Pu, J. Nam, Thin Solid Films (2007).
[6] F. Jonas, L. Schrader, Synth. Met. 41 (1991) 831–836.
[7] L. Groenendaal, F. Jonas, D. Freitag, H. Pielartzik, J. Reynolds, Adv. Mater. 12 (2000).
[8] D. Welsh, A. Kumar, E. Meijer, J. Reynolds, Adv. Mater. 11 (1999).
[9] S. Admassie, F. Zhang, A. Manoj, M. Svensson, M. Andersson, O. Inganas, Sol. Energ. Mat. Sol. C. 90 (2006) 133–141.
[10] A. Gadisa, K. Tvingstedt, S. Admassie, L. Lindell, X. Crispin, M. Andersson, W. Salaneck, O. Inganas, Synthetic Met. 156 (2006) 1102–1107.
[11] D. Wakizaka, T. Fushimi, H. Ohkita, S. Ito, Polymer 45 (2004) 8561–8565.
[12] R. Hatton, N. Blanchard, L. Tan, G. Latini, F. Cacialli, S. Silva, Org. Electron. (2009).
[13] T. Lee, Y. Chung, Adv. Funct. Mater. 18 (2008) 2246–2252.
[14] T. Lee, Y. Chung, O. Kwon, J. Park, Adv. Funct. Mater. 17 (2007) 390–396.
[15] Y. Saito, T. Kitamura, Y. Wada, S. Yanagida, Synthetic Met. 131 (2002) 185–187.
[16] K. Colladet, S. Fourier, T. Cleij, L. Lutsen, J. Gelan, D. Vanderzande, H. Neugebauer, S. Sariciftci, A. Aguirre, G. Janssen, Macromolecules 40 (2007) 65–72.
[17] Y. Kim, S. Choulis, J. Nelson, D. Bradley, S. Cook, J. Durrant, Appl. Phys. Lett. 86 (2005) 063502.
[18] Terje.A. Skotheim, Handbook of Conducting Polymer, Marcel Dekker, New york, 1998.
[19] M. Kemerink, S. Timpanaro, M. De Kok, E. Meulenkamp, F. Touwslager, J. Phys. Chem. B 108 (2004) (1882) 18820–18825.

[20] A. Higgins, S. Martin, P. Jukes, M. Geoghegan, R. Jones, S. Langridge, R. Cubitt, S. Kirchmeyer, A. Wehrum, I. Grizzi, J. Mater. Chem. 13 (2003) 2814–2818.
[21] L. Groenendaal, G. Zotti, F. Jonas, Synthetic Met. 118 (2001) 105–109.
[22] J. Kim, E. Kim, Y. Won, H. Lee, K. Suh, Synthetic Met. 139 (2003) 485–489.
[23] M. Fabretto, K. Zuber, C. Hall, P. Murphy, Macromol. Rapid Comm. 29 (2008).
[24] M. Cho, S. Kim, J. Nam, Y. Lee, Synthetic Met. 158 (2008) 865–869.
[25] Y. Ha, N. Nikolov, S. Pollack, J. Mastrangelo, B. Martin, R. Shashidhar, Adv. Funct. Mater. 14 (2004) 615–622.
[26] B. Winther-Jensen, J. Chen, K. West, G. Wallaces, Macromolecules 37 (2004) 5930–5935.
[27] S. Grecu, M. Roggenbuck, A. Opitz, W. Brutting, Org. Electron. 7 (2006) 276–286.
[28] C. Bartic, H. Jansen, A. Campitelli, S. Borghs, Org. Electron. 3 (2002) 65–72.
[29] D. Kim, P. Lee, S. Kang, K. Jang, J. Lee, M. Cho, J. Nam, Thin Solid Films (2009).
[30] Y. Xu, J. Wang, W. Sun, S. Wang, J. Power. Sources 159 (2006) 370–373.
[31] A. Sarac, G. Sonmez, F. Cebeci, J. Appl. Electrochem. 33 (2003) 295–301.
[32] K. Jang, Y. Eom, T. Lee, D. Kim, Y. Oh, H. Jung, J. Nam, A.C.S. Appl. Mater. Interfaces 1 (2009) 1567–1571.
[33] O. Levenspiel, Chemical reaction engineering, John Wiley and Sons, New York, 1962.
[34] T. Chen, X. Wu, R. Rieke, J. Am. Chem. Soc. 117 (1995) 233–244.
[35] R. Singh, J. Kumar, R. Singh, R. Kant, S. Chand, V. Kumar, Mater. Chem. Phys. 104 (2007) 390–396.
[36] L. Zhan, Z. Song, J. Zhang, J. Tang, H. Zhan, Y. Zhou, C. Zhan, Electrochim. Acta 53 (2008) 8319–8323.
[37] L. Li, Y. Huang, G. Yan, F. Liu, Z. Huang, Z. Ma, Mater. Lett. 63 (2009) 8–10.
[38] X. Vanden Eynde, P. Bertrand, Surf. Interface Anal. 27 (1999).
[39] D. Cossement, R. Gouttebaron, V. Cornet, P. Viville, M. Hecq, R. Lazzaroni, Appl. Surf. Sci. 252 (2006) 6636–6639.
[40] S. Marciniak, X. Crispin, K. Uvdal, M. Trzcinski, J. Birgerson, L. Groenendaal, F. Louwet, W. Salaneck, Synthetic Met. 141 (2004) 67–73.
[41] Y. Hsiao, W. Whang, C. Chen, Y. Chen, J. Mater. Chem. 18 (2008) 5948–5955.
[42] S. Jonsson, J. Birgerson, X. Crispin, G. Greczynski, W. Osikowicz, A. Denier van der Gon, W. Salaneck, M. Fahlman, Synthetic Met. 139 (2003) 1–10.
[43] J. Huang, P. Miller, J. Wilson, A. de Mello, J. de Mello, D. Bradley, Adv. Funct. Mater. 15 (2005) 290–296.